THE ROLE OF SPACEBORNE MILLIMETRE-WAVE RADAR IN THE GLOBAL MONITORING OF ICE CLOUD.

P.R.A. Brown[1], A.J. Illingworth[1], A.J. Heymsfield[2], G.M. McFarquhar[3], K.A. Browning[1], and M. Gosset[1]

[1] JCMM, University of Reading, UK
[2] NCAR, Boulder, CO, USA
[3] Center for Clouds, Chemistry, and Climate, Scripps Inst., La Jolla, CA, USA

Abstract

The purpose of this paper is to assess the potential of a spaceborne 94 GHz radar for providing useful measurements of the vertical distribution and water content of ice clouds on a global scale.

Calculations of longwave (LW) fluxes for a number of model ice clouds are performed. These are used to determine the minimum cloud optical depth that will cause changes in the outgoing longwave radiation (OLR) or flux divergence within a cloud layer greater than $10Wm^{-2}$ and in surface downwards LW flux greater than $5Wm^{-2}$ compared to the clear-sky value. These optical depth values are used as the definition of a "radiatively-significant" cloud. Different "thresholds of radiative significance" are calculated for each of the three radiation parameters and also for tropical and mid-latitude cirrus clouds. Extensive observational datasets of ice crystal size spectra from mid-latitude and tropical cirrus are then used to assess the capability of a radar to meet these measurement requirements. A radar with a threshold of -30 dBZ should detect 99% (92%) of "radiatively-significant" clouds in mid-latitudes (tropics). This detection efficiency may be reduced significantly for tropical clouds at very low temperatures (-80C).

The LW flux calculations are also used to establish the required accuracy within which the optical depth should be known in order to estimate LW fluxes or flux divergence to within specified limits of accuracy. Accuracy requirements are also expressed in terms of ice water content (IWC) because of the need to validate cloud parameterization schemes in General circulation Models (GCMs). We consider estimates of ice water content (IWC) derived using radar alone and also using additional information to define the mean crystal size. With crystal size information available, the IWC for samples with a horizontal scale of 1-2 km may be obtained with a bias of less than 8%. For IWC larger than $0.01gm^{-3}$, the random error is in the range +51% to -34% whereas for a value of $0.001gm^{-3}$ the random error increases to between +82% and -45%. This level of accuracy also represents the best that may be achieved for estimates of the cloud optical depth, and meets the requirements derived from LW flux calculations. In the absence of independent particle size information the bias in estimated IWC is less than 15% whilst the random error is within the range +87% and -54% for IWC greater than $0.01gm^{-3}$. This accuracy is sufficient to provide useful constraints on GCM cloud parameterization schemes.

1 INTRODUCTION

The role of clouds as a major influence on the Earth's radiation budget and therefore in the control of the global climate system is well-recognised (Senior and Mitchell 1993). The improved understanding of the climate system and predictions of climate change require that the effects of clouds on various components of the system be better described and represented in atmospheric General Circulation Models (GCMs). Of particular importance are the direct effects of clouds on the surface radiation budget and on the vertical profile of radiative heating of the atmosphere. Both have been proposed as key elements of cloud-climate feedback processes (Randall 1989, Ramanathan and Collins 1991). However, clouds also have an indirect impact on atmospheric radiation. The detrainment and subsequent evaporation of cirrus cloud from tropical convection plays a substantial role in the water vapour budget of the upper troposphere. This water vapour, in turn, has a a significant radiative effect (Lindzen 1990, Rind et al. 1991).

Global estimation of the short-wave (SW) components of the surface radiation budget (SRB) from satellite radiance measurements have shown some promise (Rieland and Stuhlmann 1993). However, estimation of the downwelling long-wave (LW) component of the SRB and atmospheric heating profiles requires the use of active sounding methods to provide the necessary measurements of cloud base and cloud top and of the liquid- or ice-water path. A frequency of 94 GHz or thereabouts has been proposed for a spaceborne cloud radar (IGPO 1994) primarily because of the sensitivity it provides, its relative freedom from atmospheric attenuation, and its compact antenna size. The primary aim of this paper is, therefore, to assess the potential of such a radar for providing global measurements of the vertical distribution of cloud condensate with accuracy sufficient to enable the determination of the associated radiation budget effects to within some defined limits.

We confine our attention here to stratiform ice clouds. We also concentrate on the consideration of LW fluxes, since it is in this area that current space-based estimates of the SRB and flux profiles are most clearly deficient and for which the determination of vertical cloud profiles and, in particular, the determination of cloud base is expected to make a significant contribution. It is recognized that, in some circumstances, the SW radiative effects of the clouds may have a more significant impact than the LW on the radiation budget terms. An example of this is tropical cirrus where, because of the large water vapour path between the cloud and the surface, the primary impact of the cloud on the SRB comes in the SW region (Ramanathan and Collins 1991). Even in this case, however, the LW effects still lead to atmospheric heating rates comparable with those generated by SW radiation and also to potentially significant dynamical effects (Starr and Cox 1985, Lilly 1988).

Some GCMs now carry cloud water content as a prognostic variable (Smith 1990, Tiedtke 1993). Various parameterizations are used to describe the cloud microphysical properties. A number of studies

have shown how sensitive the simulated climate is to variations in these cloud parameterizations (Gregory 1994, Senior and Mitchell 1993, Tiedtke et al. 1994). Changes in the cloud climatology of a GCM simulation will alter both the direct and indirect radiative effects of the clouds. A second aim of the paper is, therefore, to assess the potential of radar-derived cloud distribution measurements for the validation of GCM cloud parameterization schemes.

In Section 2 of this paper, we establish the requirements for cloud measurements both for the estimation of LW fluxes and for the validation of GCMs. We model the LW fluxes associated with a variety of ice cloud scenarios to arrive at definitions of "radiatively-significant cloud", *ie.* the minimum cloud that would alter the OLR, SRB or atmospheric heating by more than defined thresholds, and that would therefore need to be detected by a spaceborne radar. These results are also used to assess the accuracy required of the cloud measurements in order to estimate these radiation budget terms to within specified limits. We also assess changes in the ice cloud climatology of GCMs caused by changes in cloud parameterization schemes in order to assess the measurement accuracy required to validate different schemes.

In Section 3, we use extensive observational datasets of ice crystal size spectra from mid-latitude and tropical cirrus to assess how well a radar with defined operating characteristics (principally in terms of its sensitivity) will be able to meet the requirements for cloud detection and measurement accuracy derived in Section 2. We also assess the bias and spread of ice water content estimates from a single radar pulse volume.

Finally, in Section 4 we summarize the capability of spaceborne cloud radar as determined in this study, and discuss further studies needed to resolve uncertainties which have been identified.

2 ASSESSMENT OF CLOUD MEASUREMENT REQUIREMENTS.

2.1 Optical depth criterion for radiatively-significant clouds.

Vertical profiles of LW flux were calculated for a number of different ice cloud scenarios covering a range of optical depth, τ, between 0.01 and 10.0. These calculations are described in more detail by Brown et al. (1995). Based on these results, we adopt the working definition that a radiatively-significant cloud is one that causes either the OLR or flux divergence (ΔF) within a cloud layer to change by more than $10 Wm^{-2}$ or the downwelling LW flux at the surface ($F_{\downarrow}$) to change by more than $5 Wm^{-2}$ from the relevant clear-sky values. The choice of a smaller threshold for $F_{\downarrow}$ was determined by the reduced contrast in this parameter between clear-sky and optically-thick cloud cases and the desire to obtain a similar degree of resolution of this range as that for OLR. For the tropical atmosphere, a ΔF

	τ_{TRS} required for:		
	OLR	$F_{\downarrow}$	ΔF
MLW (9.5km altitude)			
CLOUD-1	0.07	0.29	
CLOUD-2	0.08	0.25	
CLOUD-3	0.08	0.23	
CLOUD-4	0.09	0.20	
MLW (4km altitude)			
CLOUD-2	0.36	0.05	0.10
TROP (16km altitude)			
CLOUD-1	0.04		0.05
CLOUD-2	0.04		0.06
CLOUD-3	0.04		0.06
CLOUD-4	0.04		0.07

Table 1: Values of the "threshold of radiative significance" (τ_{TRS}), *ie.* the minimum cloud optical depth which gives values of OLR, surface downwards LW flux, $F_{\downarrow}$, or flux divergence, ΔF, that depart by at least 10, 5, and $10 Wm^{-2}$, respectively, from the clear-sky values. Figures are given for clouds in mid-latitude winter (MLW) and tropical (TROP) standard atmospheres. In each case, CLOUD1 signifies a single 500m thick layer, CLOUD2 a 2km thick layer of uniform IWC, CLOUD3 a 2km thick layer with IWC decreasing linearly between base and top, and CLOUD4 two 1km thick layers separated in altitude by 2km.

of $10 Wm^{-2}$ over the 4km depth below the tropopause corresponds to a heating rate of $1.2 Kday^{-1}$. This is comparable in magnitude to the clear-sky heating rates in the tropical troposphere. In the mid-latitude winter atmosphere, this flux divergence corresponds to a heating rate of $0.4 Kday^{-1}$ over the same 4km region below the tropopause. This compares with clear-sky heating rates of around $-1.5 Kday^{-1}$.

From the set of LW flux calculations, we determine the minimum optical depth that will create a radiatively-significant cloud according to the above definition. This is referred to as the "threshold of radiative significance", τ_{TRS}. Different values of τ_{TRS} are derived for each of the three quantities, OLR, $F_{\downarrow}$, and ΔF and are shown in Table 1. It is evident that the most stringent criteria for cloud detection are those for tropical clouds, the criterion for OLR being closely followed by that for ΔF. Expressed in terms of IWP, and assuming a pessimistic value of $r_e = 10\mu m$, an optical depth of 0.04 corresponds to an IWP of $0.5 gm^{-2}$ or an IWC of $5 \times 10^{-4} gm^{-3}$ uniformly distributed over a 1km thick layer.

2.2 Criterion for the required accuracy of optical depth measurements.

We now seek to establish criteria for the accuracy of measurement of τ in order to estimate LW fluxes or flux divergences to within defined limits of accuracy. These limits are again chosen to be $\pm 10 Wm^{-2}$

	$\Delta\tau$ required for:		
	OLR	$F_\downarrow$	ΔF
MLW (9.5km altitude)			
CLOUD-1	0.28	0.50	
CLOUD-2	0.30	0.42	
CLOUD-3	0.31	0.42	
CLOUD-4	0.31	0.32	
MLW (4km altitude)			
CLOUD-2	1.03	0.20	0.38
TROP (16km altitude)			
CLOUD-1	0.14		0.20
CLOUD-2	0.14		0.23
CLOUD-3	0.14		0.24
CLOUD-4	0.14		0.28

Table 2: Values of $\Delta\tau$, a measurement of the required relative accuracy of measurement of the optical depth, τ, in order to specify OLR and ΔF to within $10Wm-2$, and $F_\downarrow$ to within $5Wm-2$. A value of $\Delta\tau = 0.30$ implies that τ should be measured to between +100% and −50% of the true value. Figures are given for clouds in mid-latitude winter (MLW) and tropical (TROP) standard atmospheres. The cloud layer definitions are as given in Table 1.

for OLR and ΔF and $\pm 5Wm^{-2}$ for $F_\downarrow$. We define the quantity

$$\Delta\ \tau = \frac{\Delta_G}{(\delta G/\delta(Log\tau))_{max}} \tag{1}$$

where G is one of either OLR, $F_\downarrow$, or ΔF, and Δ_G is the accuracy limit appropriate to each of these three radiation quantities. Thus, a measurement of $Log(\tau)$ falling within the range $\pm\Delta\ \tau$ of the true value will enable the LW fluxes or flux divergence to be estimated to within the required limits.

Values of $\Delta\tau$ appropriate to the estimation of OLR, $F_\downarrow$, and ΔF are shown in Table 2. It should be noted that a value of $\Delta\ \tau = 0.3$ implies that τ should be measured to within +100% and −50% of its true value. Similarly, $\Delta\ \tau = 0.15$ implies measurement to within +40% and −30%. Once again, the measurement accuracy requirements are most demanding for the estimation of OLR for the tropical cloud layers. However, existing space-based measurements of OLR already achieve an accuracy of better than the $10Wm^{-2}$ limit specified here (Barkstrom et al. 1989), and this may therefore be a less significant issue for a future spaceborne radar. The real importance of the latter lies in its potential ability to distinguish between cloud formations which produce the same OLR but which generate different downwelling fluxes and atmospheric heating rates.

2.3 Accuracy requirement for the determination of cloud altitude.

The effects of the vertical resolution of cloud radar measurements are considered in Figure 1. These show the variations in calculated LW fluxes and LW heating rates within the cloud-containing layer when a cloud of 2km thickness and an optical depth of 0.98 (an IWP of $25gm^{-2}$ for $r_e = 25\mu m$) is

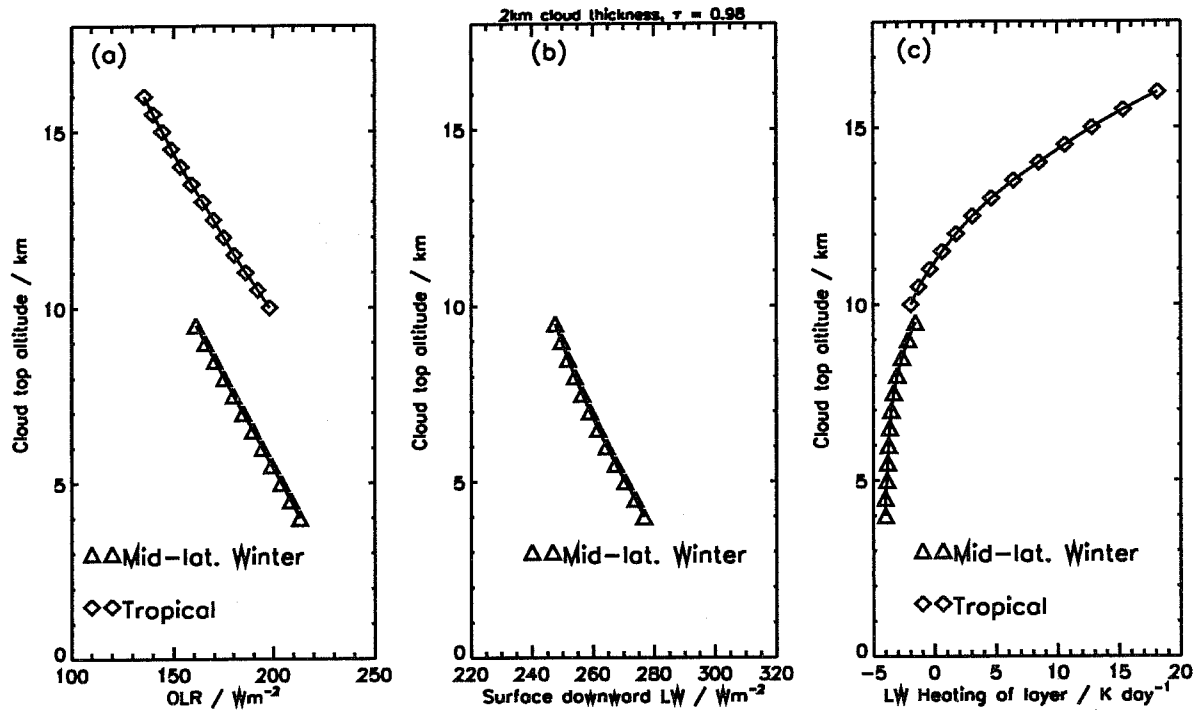

Figure 1: Variations with cloud-top altitude of (a) OLR, (b) $F_{\downarrow}$, and (c) Net LW heating rate of a cloud layer 2km thick with $\tau = 0.98$. This corresponds to an IWP of $25gm^{-2}$ for $r_e = 20.8\mu m$. Different symbols indicate the mid-latitude winter (triangles) and tropical (diamonds) atmospheres. $F_{\downarrow}$ is not shown for the tropical atmosphere in (b) since it is determined primarily by the intervening water vapour.

positioned at a range of altitudes in the tropical and mid-latitude winter atmospheres. This value of τ is in the range where the clouds are optically-thin, so that the sensitivity of the radiation budget parameters to cloud altitude will not be a maximum, but is representative of typical values for cirrus. Variations of the cloud altitude by 500m cause variations in OLR of only approximately $5Wm^{-2}$ in both tropical and mid-latitude winter cases. The surface downward LW flux in the tropical atmosphere has almost no dependance on cloud altitude due to the large water vapour path between cloud base and the surface and is, therfore, not shown in Figure 1. In the the mid-latitude winter atmosphere, the surface downward LW flux varies by approximately $3Wm^{-2}$ per 500m change in cloud (base) altitude. This value rises to around $6Wm^{-2}$ per 500m change for optically-thick cloud layers (IGPO 1994).

The sensitivity of the net LW heating rate of the 2 km layer containing the cloud is greatest for layers near the tropopause in the tropical atmosphere, with variations of approximately $3Kday^{-1}$ per 500m change in cloud altitude. The transition between net heating and net cooling of the cloud layer occurs at a cloud-top altitude of around 11 km in the tropical atmosphere. For the mid-latitude winter clouds, the maximum variation of the net LW cooling of the 2 km cloud layer is around $0.5Kday^{-1}$ per 500m change in layer altitude. For optically-thick clouds in each region, the sensitivities may be approximately double these values, ie. $6Kday^{-1}$ and $1Kday^{-1}$ per 500m step for clouds near the

tropical and mid-latitude winter tropopause, respectively (IGPO 1994). It may be noted that for the cloud with $\tau = 0.98$, the error in ΔF due to a 500m change in cloud altitude is approximately $10 W m^{-2}$. We conclude, therefore, that a measurement accuracy of 500m is consistent with the criteria discussed in sections 2.1 and 2.2.

2.4 Accuracy Of Estimates Of IWC Required To Validate GCMs.

The preceding sections have considered measurement requirements related to the direct effects of clouds on the LW radiation fluxes. For the indirect effects of clouds through their influence on the atmospheric water vapour distribution, it is difficult to establish clear criteria relating cloud measurements to the resulting radiative impact of the water vapour. However, for these processes to be modelled accurately within a GCM, it is clear that a necessary requirement is that the GCM should produce the correct cloud climatology, for example in terms of IWC. We shall therefore briefly review some GCM experiments that have demonstrated the sensitivity of zonal mean values of IWC to the microphysical details of the cloud parameterisation schemes. We shall then consider if a spaceborne radar could detect such changes in IWC and so provide validation of the various proposed schemes.

In a study of the sensitivity of the UK Meteorological Office climate model to cloud microphysics, Gregory (1994) has examined the response to changes in the parameterisation of mixed phase clouds. In one version of the UKMO model the fraction of the cloud water that is in the ice phase as opposed to supercooled water, is assumed to increase monotonically from zero at 0 C to 100% at about -15 C. Observations by Moss and Johnson (1994) suggest that the temperature at which a given ice fraction occurs should be increased by a few degrees compared with that in the version examined by Gregory. When this change was incorporated in the model Gregory found that the effect was dramatic and lead to a marked decrease in the amount of ice in the mid-latitude depression tracks during the winter at 50^o N; the zonal mean values of ice water content (IWC) at about 800mb decreased from about 0.04 to 0.01 gm^{-3}. These changes occurred in a model layer of about 100mb in thickness.

The effect of changes in the microphysics in the ECMWF model has been explored by Tiedtke et al (1994). They compared the zonally averaged mean values of IWP calculated over each model layer for two different schemes having slightly different terminal velocities for the ice particles in cirrus clouds.One scheme was based on Heymsfield and Donner (1990) in which the ice fallspeed is specified as a function of IWC and typically lies in the range $0.2 - 0.7 ms^{-1}$. The other was based on Sundqvist (1978) who specifies a constant $1 ms^{-1}$ fallspeed. The largest changes occurred in the tropics at the 300mb level where the zonal mean IWC of about 0.03 gm^{-3} was reduced by about 50%.

These two examples for ice water content - one at 300mb in the tropics, the other at 800mb in

the mid-latitude storm tracks - suggest that models are holding zonal mean values of IWC of up to 0.03 gm^{-3} (strictly, $0.1gm^{-3}$ with 30% cloud cover) and that these can change by more than +100% or -50% according to the parameterisation scheme. A spaceborne radar able to deliver this level of accuracy may therefore be of value in the validation of ice cloud parameterization schemes.

3 USE OF OBSERVED ICE CRYSTAL SIZE SPECTRA TO QUANTIFY ACCURACY OF RADAR-DERIVED IWC ESTIMATES.

In sections 2.1 and 2.2, the requirements for the detection and measurement accuracy of radiatively-significant clouds were stated in terms of optical depth, τ. Aircraft-based measurements at a single level cannot measure τ directly. We therefore relate radar reflectivity measurements to a quantity which can be measured directly, namely IWC. This has the additional advantage that IWC obtained from the integration of particle size spectra can also be validated against bulk measurements (Brown 1993, Brown and Francis 1995). In Section 4, we shall then relate the radar-derived IWC estimates to τ using the relationship given by Francis et al. (1994),

$$\tau = \frac{3\ IWP}{4\rho_{ice} r_e} \tag{2}$$

making assumptions about cloud depth and using either measured or assumed r_e.

3.1 Sources of Observational Data In Ice Clouds.

The first of the two sets of measurements discussed in this paper was obtained using the C-130 aircraft of the UK Meteorological Office. Three of the flights were a part of the field phase of the European Cloud Radiation EXperiment (EUCREX) which took place during September and October 1993. EUCREX flights sampled cirrus associated with frontal systems in the vicinity of northern Scotland. The dataset also incorporates two additional flights in frontal cirrus cloud around the UK, which were performed during April 1992. For convenience, this set of five flights is referred to as the EUCREX dataset. It comprises a total of 7900 5-second averaged size spectra (from a total of approximately 5100km of flight) measured at temperatures between -10 and -50C.

The second set of measurements was made during the Central Equatorial Pacific EXperiment (CEPEX) which took place during March and early April 1993. It sampled tropical cirrus clouds using a Learjet aircraft of Aeromet, Inc. (Heymsfield and McFarquhar 1994). This dataset comprises 11700 10-second averaged size spectra (from approximately 22800 km of horizontal flight) measured at temperatures between -10 and -65C.

Spatial scales represented by each observation are between about 500m and 2km for the range of

airspeeds of the two aircraft platforms ($100 - 200ms^{-1}$). This is comparable with the 1km cross-track footprint of a proposed spaceborne cloud radar (IGPO 1994).

For both datasets, the primary instrument used to measure ice crystal size spectra was the 2D Optical Array Probe (Knollenberg 1980). IWC was calculated from the 2D probe particle images using

$$I_{2D} = \sum_{D_{min}}^{D_{max}} n(D).M(D) \tag{3}$$

where the summation is over the range of particle size recorded by the 2D probe. The crystal mass is given by

$$M(D) = 7.38 \times 10^{-11} D^{1.9} \tag{4}$$

where M is in g and D is the crystal diameter in μm. This is equivalent to the assumption that the bulk density of quasi-spherical crystals is proportional to $D^{-1.1}$. For data which form part of the EUCREX dataset, this expression was found to give good agreement between the 2D-derived IWC and that derived using a total water content (TWC) probe (Brown and Francis 1995). It was, therefore, applied to both the EUCREX and CEPEX datasets. Details of the algorithms for the derivation of the 94GHz equivalent radar reflectivity (Z) from measured ice crystal size spectra, are described in more detail by Gosset et al. (1994).

Arnott et al. (1994) have used measurements from a crystal replicator, able to resolve crystals down to around $5\mu m$ in diameter, to show that the 2D probe does not reliably detect crystals below about $100\mu m$ in diameter. A similar conclusion was reached by Brown (1989) using holographic measurements of ice crystals. Crystals of such size are not expected to have a significant effect on the radar reflectivity. However, their effect on the total IWC may be large. The Forward Scattering Spectrometer Probe (FSSP), normally used to provide measurements of liquid cloud droplets, has been used in this study to obtain a crude estimate of the contribution to IWC from crystals below the lower size limit of the 2D probe. From CEPEX measurements, we estimate that when the total IWC is $0.001gm^{-3}$, only $20 - 40\%$ of this may be measured by the 2D probe. This estimate should, however, be regarded very much as an upper limit to the IWC due to such small crystals. This problem is not encountered within the EUCREX dataset (S Moss, personal communication). The possible implications of the underestimation of IWC by the 2D probe will be discussed further below.

3.2 Variations In Ice Particles Size Spectra As A Cause Of Error In IWC Estimation.

Scatter plots of IWC as a function of Z for each of the two datasets are shown in Figure 2. Atlas and Bartnoff (1953) and Atlas et al. (1995) show that some of the scatter present in these distributions is caused by variations in the shape of the particle size spectrum. A convenient means of expressing

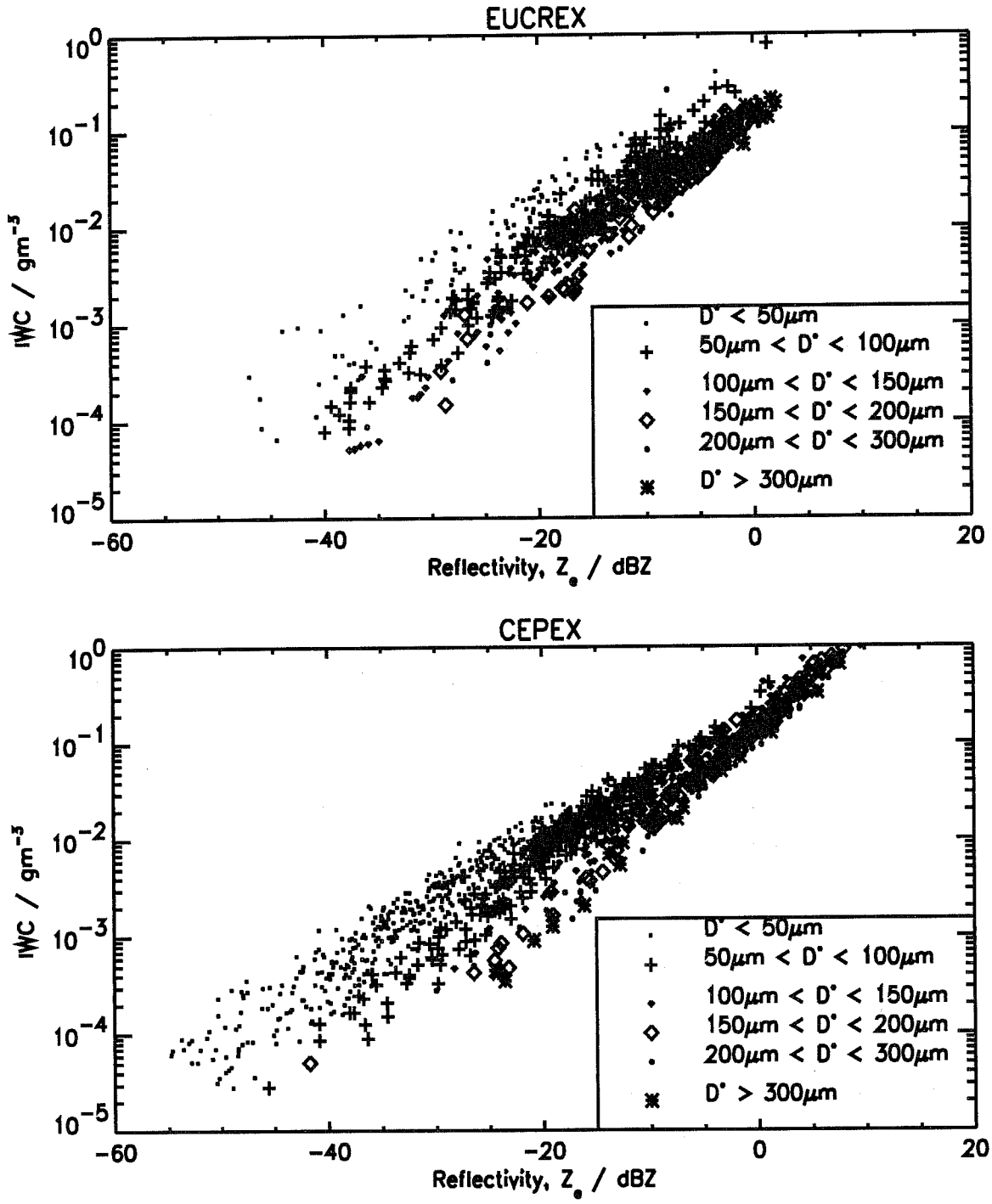

Figure 2: Scatter plots of observations of IWC and radar reflectivity, Z, calculated according to the methods of Gosset et al. (1994) for data from (a) EUCREX and (b) CEPEX. In each case, the different symbols indicate points for which the size-spectrum has a value of D^* lying within one of six different ranges. For clarity, only every tenth data point is plotted.

this variation is in terms of D^*, the scale diameter of an inverse-exponential fit to the measured size spectrum,

$$N(D) = N_0 exp(-D/D^*) \tag{5}$$

For spherical particles, IWC and Z are given by the third and sixth moments of this distribution, respectively, and it is therefore quite plausible that there will be combinations of the parameters N_0 and D^* that give the same IWC. Spectra with larger values of D^* will give higher values of Z for a given value of IWC due to the greater number of large particles present. This is illustrated by Gosset et al. (1994) and Atlas et al. (1995) and is evident in the measurements shown in Figure 2.

In simple terms, the remote sensing of the characteristics of cloud particle size spectra (ie. N_0 and D^*), using either active or passive methods, involves the use of two or more different wavelengths that have different sensitivities to particle size. Intrieri et al. (1993) describe a method based on a combination of radar and lidar backscatter measurements. They show that the radar/lidar backscatter ratio can provide particle size information in cirrus clouds, although there are constraints on the range of optical depth for which this method is suitable. The addition of such a measurement capability to a future space mission would inevitably add complexity. The main requirement is to determine surface and atmospheric radiative heating, but it is conceivable that an estimate of IWC sufficiently accurate for other purposes may be achievable using cloud radar measurements alone. In the following sections, therefore, we shall attempt to illustrate both the performance of a radar alone and the incremental improvements in measurement accuracy that might be obtained by use of additional particle size measurements. We shall also assess the impact of these accuracies on the use of cloud radar data for radiation budget studies and the validation of GCM cloud parameterization schemes.

3.3 Uncertainty in IWC for a given value of Z

The total range of IWC values at a fixed Z is large (approximately 1.5 orders of magnitude at -20 dBZ), as shown in Figure 2. The reasons for this are discussed by Atlas et al. (1995) and Gosset et al. (1994). However, a scatter plot such as this tends to mask the fact that a majority of the observations at a given Z occur within a narrower range of IWC. To obtain a more realistic view of the probable range of IWC for a given Z, we calculate the mean, $\overline{Log(IWC)}$, and standard deviation, $\sigma_{log(I)}$, of observations falling within ranges of Z of width 2.5 dBZ. For data with a log-normal distribution, as is approximately the case for the current datasets, $10^{\overline{Log(IWC)}}$ gives the most probable value, IWC_{mode} and $10^{\sigma_{log(I)}}$ gives a factor by which to multiply or divide IWC_{mode} in order to encompass 68% of the observations. For $\sigma_{log(I)} = 0.15$ this factor has a value of 1.41; therefore 68% of observations lie in the range within +41% and −29% of IWC_{mode}. For $\sigma_{log(I)} = 0.30$ the range lies between +100% and −50%.

		Z					
		$-28.75dBZ$		$-13.75dBZ$		$-3.75dBZ$	
		$\overline{Log(IWC)}$	$\sigma_{log(I)}$	$\overline{Log(IWC)}$	$\sigma_{log(I)}$	$\overline{Log(IWC)}$	$\sigma_{log(I)}$
EUCREX							
(i)	unclassified	-2.74	0.44	-1.82	0.26	-1.13	0.18
(ii)	$D^* < 50\mu m$	-2.43	0.14	-1.24	0.10		
	$50 < D^* < 100\mu m$	-3.01	0.23	-1.71	0.17	-0.82	0.16
	$100 < D^* < 150\mu m$	-3.23	0.22	-1.93	0.14	-1.04	0.14
	$150 < D^* < 200\mu m$	-3.72	0.17	-2.03	0.17	-1.16	0.16
	$200 < D^* < 300\mu m$			-2.11	0.26	-1.20	0.14
	$D^* > 300\mu m$			-1.87	0.20	-1.15	0.13
CEPEX							
(i)	unclassified	-2.72	0.31	-1.83	0.28	-1.14	0.17
(ii)	$D^* < 50\mu m$	-2.57	0.17	-1.29	0.27		
	$50 < D^* < 100\mu m$	-2.99	0.18	-1.66	0.12	-0.89	0.07
	$100 < D^* < 150\mu m$	-3.38	0.19	-1.93	0.11	-1.04	0.09
	$150 < D^* < 200\mu m$	-3.57	0.12	-2.16	0.10	-1.19	0.10
	$200 < D^* < 300\mu m$			-2.32	0.11	-1.29	0.10
	$D^* > 300\mu m$					-1.27	0.12

Table 3: Means ($\overline{Log(IWC)}$) and standard deviations ($\sigma_{log(I)}$) of observations of $Log(IWC)$ for data points lying within 2.5 dBZ ranges of Z centred on the indicated values (i) with no classification by temperature or D^*, and (ii) for observations stratified by means of various ranges of D^*. The interpretation of $\sigma_{log(I)}$ is described in the text. Blank entries in the table indicate that there were fewer than 20 samples with that combination of Z and D^*.

Values of $\overline{Log(IWC)}$ and $\sigma_{log(I)}$ are shown in Table 3 for three representative values of Z. For each dataset, two sets of values are given: (i) values based on all observations without any stratification of the data, and (ii) values based on observations that have been sorted into six ranges of D^*. Stratification of the data using D^* follows the theoretical treatment of Atlas et al. (1995) and Gosset et al. (1994), showing that both IWC and D^* or some other characteristic particle size are needed to specify Z tightly.

The main points to note from Table 3 are that the mean values of $Log(IWC)$ for a given Z in the two datasets are broadly similar and that in the majority of cases, $\sigma_{log(I)}$ is less than 0.30 (ie. data in the range +100% to -50% of the mode). This is further emphasised in Figure 3 which shows $\overline{Log(IWC)}$ and $\sigma_{log(I)}$ in each 2.5 dBZ interval between -50 and +10 dBZ. For $-30 < Z < +5$ dBZ, the maximum difference in $\overline{Log(IWC)}$ between EUCREX and CEPEX is 0.17, corresponding to a difference in IWC of 48%, but with most values being much less than this. For $Z < -30$ dBZ, differences in $\overline{Log(IWC)}$ between the two datasets result primarily from differences in the range of

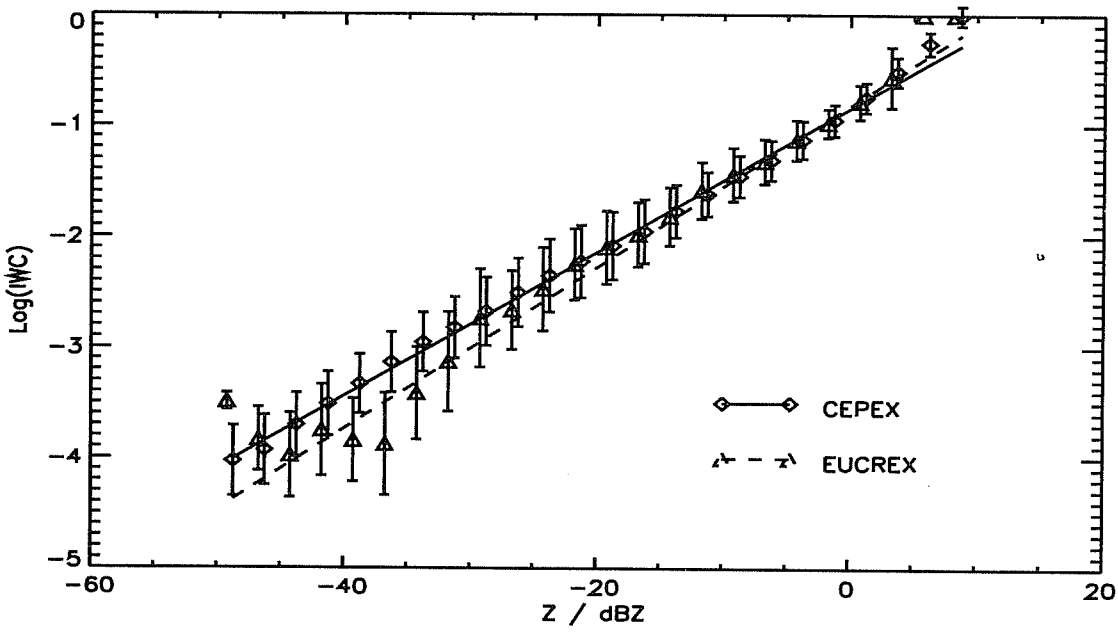

Figure 3: The mean values of $Log(IWC)$ for data falling within 2.5 dBZ ranges of Z. The error bars indicate plus and minus one standard deviation. CEPEX data are plotted at the centre of each 2.5 dBZ interval with EUCREX data offset slightly for clarity. The curves show the least-squares fit curves, $Log(IWC) = aZ + b$ for each complete dataset.

values of D^* included in the data sample. In this range of Z, the CEPEX data have D^* predominantly less than $100\mu m$ whereas the EUCREX data have a wider spread of D^*. Thus the CEPEX data have, on average, a higher IWC for a given Z. The extent to which this represents real differences in the microphysics of the clouds in these two datasets or merely the sampling of clouds over different ranges of altitude and temperature and with different life histories is unknown. This question will, however, require further study if $Z - IWC$ relationships applicable to all regions of the globe are to be obtained.

The classification of observations using the measured value of D^* generally results in a significant reduction in $\sigma_{log(I)}$ and hence the uncertainty in IWC. Differences in $\overline{Log(IWC)}$ between the two datasets for any one D^* class are, in the majority of cases less than 0.14, corresponding to differences in IWC of 40%. Within each dataset, classification by means of the -40C temperature threshold can lead to a subset of the the observations having a slightly reduced uncertainty, although the other subset at each reflectivity then has an uncertainty increased by a comparable amount.

A further point to note from Table 3 is the reduction in $\sigma_{log(I)}$ for unclassified data as Z increases. This arises through the combined effects of Mie scattering and the assumed decrease of crystal bulk density with diameter in limiting Z as D^* increases (Gosset et al. 1994). In both datasets, the observations at higher Z tend also to have higher D^*, and thus fall into a narrower range of IWC. Our conclusions here differ somewhat from those of Atlas et al (1995). They assume a constant bulk density for all crystals which gives a broader range of IWC at fixed Z. Since many of our subsequent

conclusions about the radar capability depend strongly on the relatively small scatter of IWC values at fixed Z, the validation of the theoretically-derived Z will be a key use for the ground- and aircraft-based millimetre-wave radars which are now coming into use. The simultaneous and independent measurement of IWC will also be a key feature of such studies.

3.4 Accuracy of IWC estimates derived from Z.

We now derive estimates of the IWC using the calculated values of Z. The latter are taken as a proxy for actual cloud radar observations. We calculate two different estimates, (i) from Z alone, this being referred to as IWC_Z, and (ii) from a combination of measurements of Z and D^* to obtain a value of IWC_{Z,D^*}. Where the discussion refers in general terms to the IWC derived by either of these three methods, we will term this IWC_{estim} as opposed to the true measured value, IWC_{true}.

For each dataset, all observations were ranked contiguously day-by-day and run-by-run. Only the first 2000 of the 7900 ranked EUCREX observations and the first 3000 of the 11700 ranked CEPEX observations were used to derive functional relationships between $Log(IWC)$ and Z. These functions were then applied to all observations within each dataset to derive the estimated IWC, so as to test their representativeness. Atlas et al. (1995) suggest that for a particular experiment location, there may be systematic changes on a day-to-day basis in the bulk relationships between IWC and Z (ie. when these are unstratified by any other data input such as D^*). By using only a part of each dataset to derive $IWC - Z$ relationships, our approach is designed to accommodate the effect of such changes and to identify any possible biases that they might introduce in IWC_{estim}.

3.4.1 Derivation of IWC_Z

The relationship used in the case of the EUCREX dataset was a simple linear least-squares fit of $Log(IWC)$ as a function of Z, ie.

$$Log_{10}(IWC_Z) = aZ + b \tag{6}$$

The parameters a and b of this function are shown in Table 4 for both the datasets. For the CEPEX dataset, however, the simple fit shown in Table 4 was replaced by an interpolation between the mean values of $Log(IWC)$ in each 2.5 dBZ range of Z. This interpolation was used because the CEPEX dataset contains a significant number of observations at IWC values between 0.1 and 1 gm^{-3} which have values of D^* mostly exceeding $150\mu m$. The effects of Mie scattering in limiting the range of values of Z for a given IWC within this range (see Figure 2(b)) are such that a simple linear fit to the CEPEX data is inappropriate. The problem was also apparent for EUCREX data but because of the relative lack of samples in this high-IWC and high-D^* region, the interpolation method was not found

		a	b
EUCREX (i)	unclassified	0.074	-0.814
(ii)	$D^* < 50\mu m$	0.083	-0.097
	$50 < D^* < 100\mu m$	0.088	-0.487
	$100 < D^* < 150\mu m$	0.090	-0.736
	$150 < D^* < 200\mu m$	0.095	-0.793
	$200 < D^* < 300\mu m$	0.091	-0.883
	$D^* > 300\mu m$	0.078	-0.754
CEPEX (i)	unclassified	0.066	-0.795
(ii)	$D^* < 50\mu m$	0.076	-0.334
	$50 < D^* < 100\mu m$	0.086	-0.480
	$100 < D^* < 150\mu m$	0.095	-0.668
	$150 < D^* < 200\mu m$	0.095	-0.835
	$200 < D^* < 300\mu m$	0.095	-0.901
	$D^* > 300\mu m$	0.108	-0.851

Table 4: Coefficients a and b of the least squares-fit, $Log_{10}(IWC) = aZ + b$.

to provide any significant improvement on the simple linear fit.

3.4.2 Derivation of IWC_{Z,D^*}.

In both datasets, linear least-squares fits of $Log(IWC)$ as a function of Z were calculated for observations in six classes of D^*, the fit parameters being as shown in Table 4. It is noted that the maximum values of a approach the theoretical maximum of 0.1 which would be obtained for a perfect inverse-exponential size spectrum (Atlas et al. 1995, Gosset et al. 1994). There is good agreement between the fit parameters derived from the two datasets for the same D^* class. Differences in IWC for a fixed value of Z only exceed 25% in circumstances in which one or other dataset has a relatively small sample size eg. for $D^* < 50\mu m$ and $Z > -10dBZ$ where the CEPEX dataset has a small sample size compared to that of the EUCREX dataset. The observed value of D^* is used to assign an observation to one of the six classes, and therefore to select the appropriate set of fit parameters from which to calculate IWC_{Z,D^*}.

3.4.3 Comparison of the performance of different IWC estimates.

Estimated values of IWC using the two methods described in Sections 3.4.1 and 3.4.2 are shown as a function of the measured IWC in Figure 4. In both the EUCREX and CEPEX datasets, IWC_{Z,D^*} shows a lower degree of scatter than IWC_Z. In the context in which measurements of Z are to be used, namely the estimation of radiation budget parameters, it is necessary to assess quantitatively

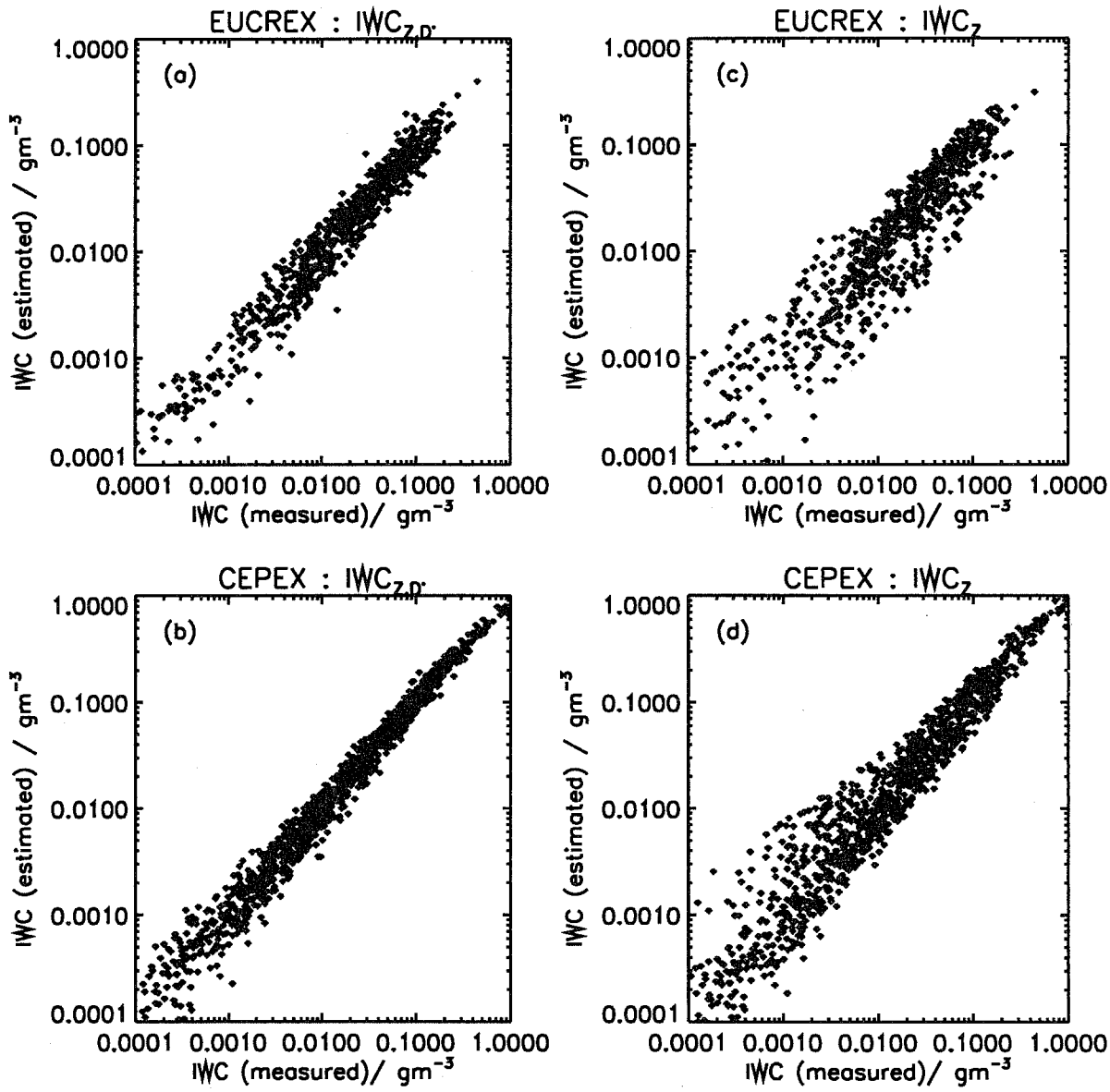

Figure 4: Scatter plots of IWC estimated from a measurement of Z against measured IWC. (a) and (b) show data from EUCREX and CEPEX, respectively, in which the observed value of D^* has been used to select the most appropriate Log(IWC)-Z regression (IWC_{Z,D^*}), whilst (c) and (d) show estimates derived using Z only (IWC_Z), as described in the text. For clarity, only every tenth data point is plotted.

	Method	IWC_{true}	$\sigma_{log(I)}$	$\frac{IWC_{estim}}{IWC_{true}}$
EUCREX	IWC_{Z,D^*}	1.3×10^{-3}	0.26	1.06
$\Delta\tau = 0.32$		1.3×10^{-2}	0.18	0.95
(z = 9.5km)		7.5×10^{-2}	0.15	0.93
$\Delta\tau = 0.20$	IWC_Z	1.3×10^{-3}	0.38	1.15
(z = 4.0km)		1.3×10^{-2}	0.27	0.89
		7.5×10^{-2}	0.24	0.88
CEPEX	IWC_{Z,D^*}	1.3×10^{-3}	0.19	1.01
$\Delta\tau = 0.20$		1.3×10^{-2}	0.14	0.96
		1.3×10^{-1}	0.10	1.03
	IWC_Z	1.3×10^{-3}	0.37	1.20
		1.3×10^{-2}	0.20	0.97
		1.3×10^{-1}	0.15	1.02

Table 5: Values of $\sigma_{Log(I)}$, the standard deviation of $Log(IWC_{estim})$, for groups of observation having values of $Log(IWC_{true})$ lying in bands of width 0.25. The table also shows the ratio of IWC_{estim}/IWC_{true}. The measurement requirements, $\Delta\tau$ are taken from the worst cases shown in Table 2 for either $F_{\downarrow}$ or ΔF.

both the random and bias errors in IWC estimates. As noted previously, the kind of presentation in Figure 4 accentuates the scatter and tends to mask the fact that a majority of the data lie within a narrower range. Thus, we shall again calculate means and standard deviations of $Log(IWC_{estim})$ as a function of $Log(IWC_{true})$, assuming an approximate log-normal distribution in IWC_{estim}. These are shown in Figure 5, and a selection of representative values is tabulated in Table 5.

From Figure 5 and Table 5, we can draw the following main conclusions applicable to both datasets for samples representing a horizontal average of approximately 1-2 km and with IWC greater than $0.01gm^{-3}$. (i) If Z alone is measured, then the random error in values of IWC_Z is within the range +86% to −46%. (ii) If Z and D^* are known, the error in IWC_{Z,D^*} is reduced to within the range +51% to −34%. (iii) The bias in the mean value of IWC_Z derived from many observations of Z alone is less than 12%. For IWC_{Z,D^*}, this bias is reduced to about 7%. Somewhat larger bias and random errors occur for lower values of IWC_{true}.

4 CLOUD RADAR MEASUREMENT CAPABILITIES IN RELATION TO REQUIREMENTS.

We first seek to reconcile the measurement requirements (from Section 2) derived in terms of optical depth with the capabilities (from Section 3) described in terms of IWC. It is clear from Equation (2) that a measurement of τ requires knowledge of both IWC and r_e. In the derivation of IWC_{Z,D^*}, it is implicit that a measurement of D^* is available, from which r_e may also be estimated. The error

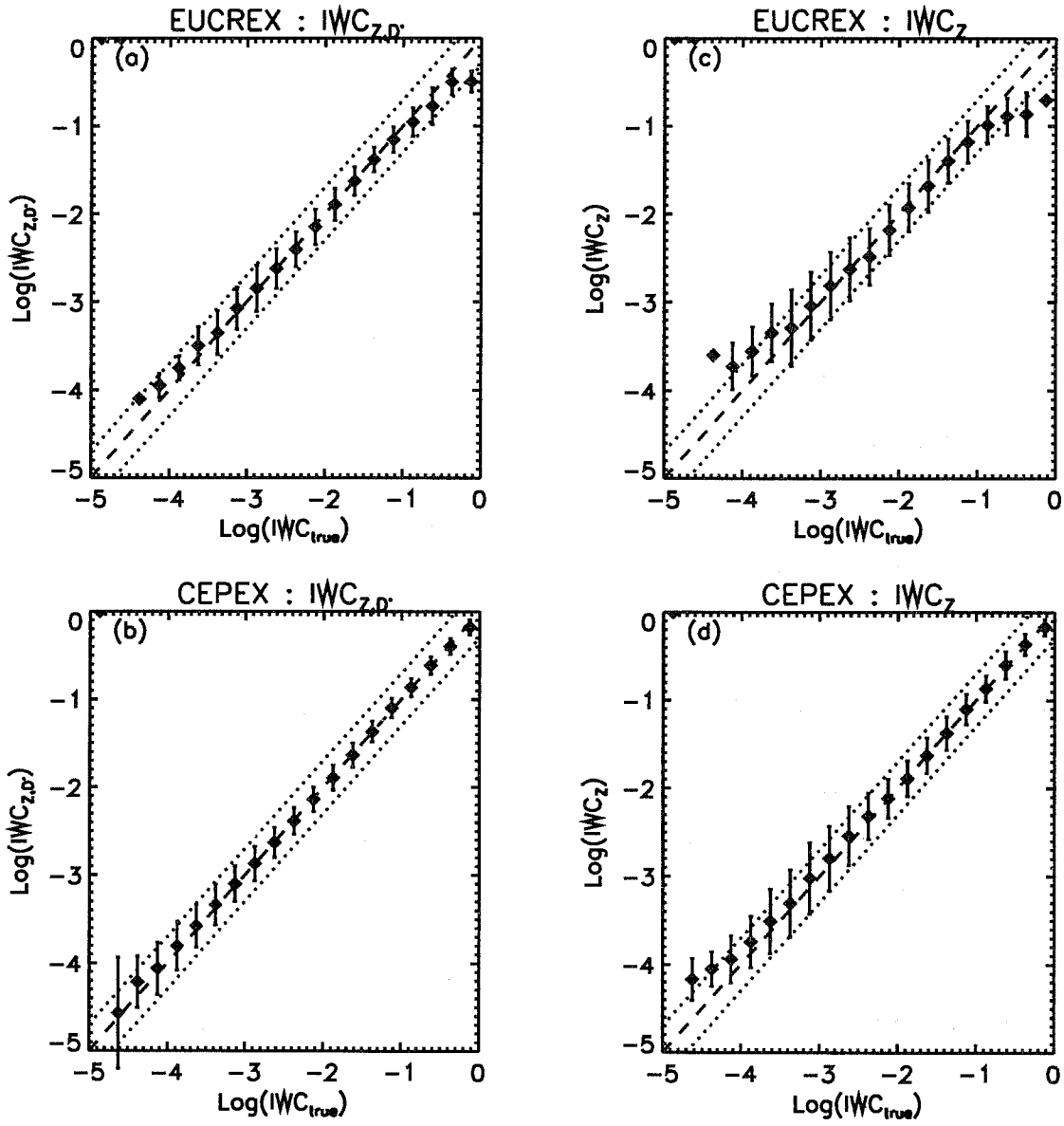

Figure 5: The points and error bars show the mean and standard deviation of $Log(IWC_{estim})$ for all observations falling within ranges of $Log(IWC_{true})$ of 0.25. As in Figure 8, (a) and (b) show data from EUCREX and CEPEX, respectively, for IWC_{Z,D^*}, whilst (c) and (d) show IWC_Z, these two estimates being derived as described in the text. The dotted lines indicate the range inside which IWC_{estim} is within +100% and -50% of IWC_{true}.

estimates for IWC_{Z,D^*} therefore represent the best possible accuracy for τ. A full assessment of the accuracy of τ must await the knowledge of the error characteristics of the D^* (or r_e) measurement. Because they include no knowledge of r_e, our estimates of IWC_Z cannot be related directly to τ or cloud radiative properties. We will, however, still seek to examine their applicability to the validation of GCM ice cloud climatology.

4.1 Detectability of ice clouds.

We have, in Section 2, defined a radiatively significant cloud as one which changes OLR or ΔF (LW flux divergence within a cloud layer) by more than $10 Wm^{-2}$ or which changes $F_{\downarrow}$ (the surface downwards LW flux) by more than $5 Wm^{-2}$, all three of these parameters being taken relative to the clear sky values. Table 1 gives the values of τ_{TRS}, the minimum optical depth that will constitute a radiatively-significant cloud for the range of modelled cloud scenarios. We now use the values of IWC, Z, and D^* from the two observational datasets in Section 3 to estimate the fraction of radiatively-significant clouds that would be detected by a radar with a given sensitivity threshold. We assume that each observation is representative of a 1 km-thick cloud layer with a uniform distribution of IWC and D^* in the vertical and calculate the optical depth, τ_{est}, of such a layer. By combining *measured* values of IWC and D^* in this estimate of τ, there is no conflict with the inability, described previously, to estimate τ from radar measurements alone.

For an inverse-exponential size distribution of quasi-spherical ice crystals, the effective radius, $r_e = 1.5\ D^*$. Thus, from (1), the optical depth of a 1km thick cloud is given by

$$\tau_{est} = \frac{3}{4}\ \frac{1000.\ IWC}{1.5\ D^*\ \rho_{ice}} \tag{7}$$

We may then determine the detection efficiency from the fraction of observations with $\tau_{est} > \tau_{TRS}$ for which Z is also greater than the radar threshold. We test EUCREX data against τ_{TRS} values which are the minima of the various values determined for the mid-latitude winter atmosphere in Table 1. Similarly, CEPEX data are tested against minima of the τ_{TRS} values calculated for the tropical atmosphere. The results are shown in Table 6 for three different radar sensitivity thresholds.

Arnott et al. (1994) suggest that, due to a combination of the detection of smaller crystals and undercounting by the 2D probe in the size range $25 - 100\mu m$, it may be common for absorption cross-sections, and hence optical depths to be a factor of two larger than would be deduced from 2D probe data alone. We have therefore made a further estimate of the cloud detection efficiency, assuming the value of τ_{est} to be double that obtained from (7). These results are shown in brackets in Table 6.

The figures in Table 6 suggest that a radar with a threshold of -30 dBZ would be a highly-efficient detector of radiatively-significant mid-latitude cirrus. This applies even in the event that the cloud

	-40 dBZ	-30 dBZ	-20 dBZ
EUCREX, MLW			
OLR (τ_{TRS}=0.07)	100.0 (99.8)	99.3 (98.6)	91.6 (87.0)
$F_{\downarrow}$ (τ_{TRS}=0.09)	100.0 (99.8)	99.5 (98.8)	92.2 (87.9)
CEPEX, TROP			
OLR (τ_{TRS}=0.04)	99.9 (99.3)	95.7 (90.2)	76.2 (68.6)
ΔF (τ_{TRS}=0.05)	99.9 (99.6)	97.2 (92.0)	78.8 (70.7)

Table 6: The figures in the table show the percentage of observations which have an estimated optical depth exceeding the τ_{TRS} and which also exceed the three different thresholds of radar reflectivity. τ_{TRS} values are taken from Table 1. The figures in brackets assume that the optical depth is double what would be estimated from 2D probe data.

optical depths are double those deduced from 2D probe data alone. For a radar threshold of -20 dBZ, the detection efficiency falls significantly, such that around 10% of radiatively-significant cloud may not be detected.

For the CEPEX dataset, a radar threshold of -30 dBZ remains an efficient detector of radiatively-significant cloud provided that the 2D probe-derived estimate of optical depth is valid. However, even in the event of the optical depth being double these estimates, it would still detect around 92% of clouds that have a significant impact on the LW heating of the upper troposphere.

These conclusions differ somewhat from those of Atlas et al. (1995). Our approach has been to consider only the fraction of data points that represent $\tau > \tau_{TRS}$ and then to determine what fraction of these also have Z exceeding a chosen threshold. Atlas et al., on the other hand, note that a significant fraction of cloud observations have Z less than a -30 dBZ threshold and then note that some of these undetected points are radiatively-significant.

Knollenberg et al. (1993) have reported microphysical measurements of tropical cirrus anvils at temperatures down to -80C, significantly colder than the minimum of around -65C in the CEPEX dataset. A notable characteristic of these measurements is that the IWC was commonly concentrated in the size range $5 - 50\mu m$, again lower than the majority of the CEPEX data. Since these very small crystals contribute the major part of the optical depth, but generate only very low radar reflectivities, it is possible that the detection efficiency of a -30 dBZ radar would fall further below the values

deduced from the CEPEX dataset. This is an extreme case of the underestimation of IWC in 2D probe data that was noted in section 3.1. There is a clear need for further measurements in such very cold tropical cirrus in order to verify the definition of radiative significance and the ability of a radar of a given threshold to detect them. It is also necessary to ascertain the horizontal and vertical extents of such small-particle regions and to quantify possible errors that might be introduced into the assignment of, for example, cloud top heights if they are found to overlay deeper regions of detectable cloud.

It must be borne in mind that the calculations in this section remain a very limited estimate of cloud detectability because they are founded on two particular premises. The first is that the aircraft measurements, which are 5- or 10-second averages along the aircraft track, are representative of cloud volumes of the order of $1km^3$ which might constitute a typical radar pulse volume viewed from space. The second is that they assume that the distribution of data points in the IWC-Z space, or any similar data space, is identical in our datasets to the actual cloud climatology. There are several reasons why the latter might not be true, not the least of which is that aircraft missions such as those in EUCREX, which are designed to sample cloud microphysical properties, tend to concentrate on the regions where the cloud occurs. Thus, it is by no means certain that the resulting observations will have sampled optically-thick, optically-thin, warmer, or colder clouds with the same frequency with which they actually occurred within the experimental region. A full consideration of the detectability of radiatively-significant cloud by radar must therefore await the outcome of long-duration ground-based measurements of ice clouds using combinations of cloud radar and radiation flux measurements. Such measurements are now possible or planned at a number of locations.

4.2 Accuracy of estimation of LW fluxes

As noted earlier, we take the value of $\sigma_{log(I)}$ derived from estimates of IWC_{Z,D^*} as an estimate of the best possible accuracy of $log\tau$. It was observed in Section 2.2 that the most stringent measurement accuracy requirements occur for the estimation of OLR. However, since OLR is already measured with $\pm 10 Wm^{-2}$ accuracy, it is more useful to compare the radar capability against the requirements for $F_{\downarrow}$ and ΔF. The worst-case requirements for $\Delta\tau$ for each of these two quantities obtained from Table 2 are restated in Table 5.

We see from this comparison that for mid-latitude clouds at tropopause-level, IWC_{Z,D^*} achieves the desired accuracy for all purposes, $\sigma_{log(I)}$ always being less than the minimum requirement of $\Delta\tau = 0.32$. For low-level mid-latitude clouds, the requirement of $\Delta\tau = 0.20$ will probably be met in most circumstances, since the IWC of these clouds is likely to lie in the upper part of the range shown in Table 5. For the tropical clouds, IWC_{Z,D^*} achieves sufficient accuracy for the estimation of ΔF

across the whole range of IWC.

4.3 Validation of GCM cloud parameterization schemes.

From the discussion of GCM experiments in section 2.4, it was evident that the ability to measure zonal mean IWC over typical model layer thicknesses to an accuracy of 50% or better would be just about sufficient for the validation of GCM ice cloud parameterization schemes. To compare the radar capabilities against this requirement, it is most appropriate to consider the bias identified in the ratio of IWC_{estim}/IWC_{true} (the last column of Table 5) since this represents a systematic error in the mean of many observations. It is evident that the bias in IWC_{estim} is less than 20% in all cases, with IWC_{Z,D^*} generally showing the best performance. Thus it possible that cloud radar data alone may provide measurements of time- and space-averaged IWC that meet the main requirement. Further consideration of errors in radar-derived cloud measurements due to sampling strategies is outside the scope of this paper.

5 SUMMARY AND CONCLUDING REMARKS.

The purpose of this paper is to examine some of the requirements for global-scale measurements of ice clouds, and to assess the capability of a spaceborne millimetre-wave radar to meet them.

The first step in the paper is to establish benchmarks for radiatively-significant clouds and the measurement accuracies required:

- We define radiatively-significant clouds as those which cause departures from clear-sky values of $10Wm^{-2}$ or more in OLR, $10Wm^{-2}$ or more in the LW flux divergence within a cloud layer, or $5Wm^{-2}$ in the surface downwelling LW flux. This value of LW flux divergence corresponds to a heating rate of $1.2Kday^{-1}$ for the 4km layer below the tropical tropopause.
- We define the requirement for the accuracy of measurement of cloud optical depth as that needed to estimate these LW radiation quantities to within the same limits.
- Different schemes for the parameterization of layer cloud in GCMs can lead to changes in zonally-averaged IWC which exceed +100% and -50% and a measurement accuracy in terms of IWC is required that matches this.

We then examine a number of mid-latitude and tropical ice cloud scenarios and, taking the worst-case scenarios (*ie.* the ones that are most demanding in terms of measurement capability), we find that:

- Clouds which are radiatively-significant for LW flux divergence have optical depth exceeding 0.05

(an IWP of $0.63gm^{-2}$ for $r_e = 10\mu m$) and require it to be measured to within +58% and -37% of the true value.

• Clouds which are radiatively-significant for the surface downwelling LW flux have optical depth exceeding 0.20 (an IWP of $2.50gm^{-2}$ for $r_e = 10\mu m$) and require it to be measured to within +100% and -50%.

• Clouds which are radiatively-significant for OLR have optical depth exceeding 0.04 (an IWP of $0.50gm^{-2}$ for $r_e = 10\mu m$) and require it to be measured to within +38% and -28% of the true value. Although this this is a more stringent requirement than those in the two preceding bullets, we do not regard the estimation of OLR as the primary task of a cloud radar.

An analysis of some aircraft measurements of ice particle size distributions in cirrus clouds in mid-latitudes and the tropics has been carried out to estimate their radar properties. An ice density that was approximately inversely proportional to the diameter was used because this gave the best agreement with bulk IWC measurements for the mid-latitude cirrus (Brown and Francis 1995). On this basis, we conclude that a spaceborne cloud radar would yield the following information:

(a) Detectability of cirrus

• A radar with a threshold of -30dBZ would detect 99% of mid- latitude cirrus and 92-97% of tropical cirrus clouds defined to be radiatively significant for estimation of LW flux divergence and surface LW flux.

• The detection efficiency for tropical cloud may be increased to 99% by decreasing the radar threshold to -40 dBZ. The detection efficiency of tropical cirrus at extremely low temperatures of around -80C may be lower than these figures.

• The use of co-located lidar measurements as a means of detecting the very cold tropical cirrus may be a more cost-effective strategy than using a more sensitive radar.

• Reduction of the radar threshold to -20 dBZ would mean that around 10% of radiatively-significant mid-latitude cirrus and 20-30% of similar tropical cirrus would be undetected.

(b) Accuracy of measurement.

• If the radar measurement of Z is supplemented by a measurement of mean ice particle size (D^*), such as might be provided by co-located lidar backscatter measurements (Intrieri et al. 1993), then, for a 1km cloud sample with IWC exceeding $0.013gm^{-2}$, the random error in the estimated value of IWC is between +50% and -34%. The bias in the mean of many estimates of IWC is less than ±8%.

• With D^* known, the cloud optical depth may also be determined to within this same range of accuracy. This capability meets all requirements for measurement accuracy except for the estimation of OLR from tropical cirrus.

• If the radar measurement of Z is used alone, then the random error in IWC estimates would be within the range +85% to -46%, with a bias of less than ±18%. This provides sufficient accuracy for

the validation of GCM ice cloud climatology.

• Since OLR has the greatest sensitivity to changes in IWP, the use of measured OLR to further constrain the IWP when the cloud geometry has been determined by the radar needs further study.

(c) Geographical biases.

Particular differences in the response of the radar for the two observational datasets used in this study are:

• When Z is below -30 dBZ then, for a given value of Z, the tropical cirrus have an IWC larger by up to a factor of two compared to the mid-latitude cirrus. The difference is much less for Z in the range -30 to +5 dBZ. This suggests the possibility that globally-applicable IWC-Z relationships appropriate to the estimation of area- and/or time-mean IWC may eventually be derived.

• The best-fit IWC-Z relationships derived for each D^* class are very similar for tropical and midlatitude cirrus. For D^* in the range $50 - 100\mu m$, for a given Z the tropical values of IWC are only up to 15% higher than those from the midlatitudes. For D^* in the range $200 - 300\mu m$ the differences increase from zero for a Z of 0dBZ to about 25% for a Z of -10dBZ.

Any conclusions concerning the ability of the proposed spaceborne cloud radar to detect and quantify clouds are dependant on the validation of the algorithms used to determine the radar reflectivity of ice clouds from aircraft-measured crystal size spectra. This is particularly important for cloud regions with large values of D^*, *ie.* a larger proportion of larger crystals, for which the combined effects of Mie scattering and the assumed decrease in crystal bulk density with diameter become increasingly important in limiting the value of Z (Gosset et al. 1994). There is thus a need for in-situ observations of cirrus particle size spectra that are closely co-located in time and space with 94 GHz radar observations. With the kind of spatial variability that has been observed in cirrus on space scales of a few hundred metres or less, the requirements for co-location are quite strict, and may be met best by an aircraft-mounted radar system able to view along the aircraft flight path. Such field measurements, preferably also with co-located lidar and LW radiation observations, should be a priority for development work with 94 GHz radar systems in the near future.

Acknowledgements

The EUCREX measurement campaign was funded by the Climate programme of the Commission Of The European Communities under contract EV5V-CT92-0130. We thank staff from the Meteorological Research Flight, in particular Sarah Moss and Helen Greensmith, for their assistance in the processing and provision of data from the EUCREX field campaign. The analysis of the CEPEX data at SIO was sponsored in part under NSF grant NSF-8920119. Work on the calculation of 94GHz reflectivity was supported by NERC grant GR3/8765. We would like to acknowledge the numerous discussions that have contributed to parts of this paper, in particular comments from David Atlas,

Peter Francis, Keith Shine, and Tony Slingo.

References

Atlas D, S Y Matrosov, A J Heymsfield, M D Chou, and D B Wolff(1995) Radar and radiation properties of ice clouds. *submitted to* J.Appl.Met.

Arnott W P, Y Y Dong, and J Hallett (1994) Role of small ice crystals in radiative properties of cirrus: A case study, FIRE-II, 22 Nov. 1991. J.Geophys.Res., 99, D1, 1371-1381.

Barkstrom B R, E Harrison, G Smith, R Green, J Kibler, R Cess and the ERBE Science Team (1989) Earth Radiation Budget Experiment (ERBE) archival and April 1985 results. Bull.Amer.Meteor.Soc., 70, 1254-1262.

Brown P R A (1993) Measurements of the ice water content of cirrus using an evaporative technique. J.Atmos.Oceanic Technol., 10:, 579-590.

Brown P R A and Francis P N (1995) Improved measurement of the ice water content in cirrus using a total water evaporator. J.Atmos.Oceanic Technol. (in press)

Brown P R A, A J Illingworth, A J Heymsfield, G M McFarquhar, K A Browning, and M Gosset (1995) The role of spaceborne cloud radar in the global monitoring of ice cloud. *submitted to* J.Appl.Met.

Francis P N, A Jones, R W Saunders, K P Shine, A Slingo, and Z Sun (1994) An observational and theoretical study of the radiative properties of cirrus: Some results from ICE'89. Quart.J.Roy.Met.Soc., 120, 809-848

Gosset M, A J Illingworth, P R A Brown, and J Thomason (1994) (manuscript in preparation).

Gregory D (1994) Sensitivity of climate simulation to parameterisation of mixed phase cloud. (manuscript in preparation)

Heymsfield A J and L J Donner (1990) A scheme for parameterising ice cloud water content in general circulation models. J.Atmos.Sci., 47, 1865-1877.

Heymsfield A J and G M McFarquhar (1994) A dedicated microphysics mission during the Central Equatorial Pacific Experiment (CEPEX). Amer.Met.Soc., 8th Conf. On Atmos. Radiation, 23-28 Jan.1994, Nashville.

IGPO (1994) Utility and feasibility of a cloud profiling radar. IGPO Publication Series No. 10, International GEWEX Program Office.

Intrieri J M, G L Stephens, W L Eberhard, and T Uttal (1993) A method for determining cirrus cloud particle sizes using lidar and radar backscatter techniques. J.Appl.Met., 32, 1074-1082.

Knollenberg,R.G. (1980) Techniques for probing cloud microstructure. in Clouds: their formation, optical properties and effects. pp.15-91 (ed. P.V.Hobbs and A.Deepak)

Knollenberg R G, K Kelly, and J C Wilson (1993) Measurements of high number densities of ice crystals in the tops of tropical cumulonimbus. J.Geophys.Res., 98, D5, 8639-8664.

Lilly D K, (1988) Cirrus outflow dynamics. J.Atmos.Sci., 45:, 1594-1605.

Lindzen R S, (1990) Some coolness regarding global warming. Bull.Amer.Met.Soc., 71:, pp288-299

Moss S J and Johnson D W (1994) Aircraft measurements to validate and improve numerical model parameterisation of ice to water ratio in clouds. Atmos.Research (to be published)

Ramanathan V and W Collins (1991) Thermodynamic regulation of ocean warming by cirrus clouds deduced from observations of the 1987 El Nino. Nature, 351, 27-32.

Randall D A (1989) Interactions among radiation, convection, and large-scale dynamics in a general circulation model. J.Atmos.Sci., 46, 1943-1970

Rieland M and R Stuhlmann (1993) Toward the influence of clouds on the shortwave radiation budget of the Earth-Atmosphere system estimated from satellite data. J.Appl.Met., 32, 825-843

Rind D, E-W Chiou, W Chu, J Larsen, S Oltmans, J Lerner, M P McCormick, and L McMaster (1991) Positive water vapour feedback in climate models confirmed by satellite data. Nature, 349:, pp500-503

Senior C A and Mitchell J F B (1993) Carbon Dioxide and Climate: The impact of Cloud Parameterization. J.Climate, 6, 393-418.

Smith R N B (1990) A scheme for predicting layer clouds and their water content in a general circulation model. Quart.J.Royal Met.Soc., 116, 435-460.

Starr D O'C and S K Cox (1985) Cirrus clouds. Part II. Numerical experiments on the formation and maintenance of cirrus. J.Atmos.Sci., 42, 2663-2681.

Sundqvist H (1978) A parameterisation scheme for non-convective condensation including prediction of cloud water content. Quart.J.Royal Met.Soc., 104, 677-690.

Tiedtke M (1993) Representation of clouds in large-scale models. Monthly Weather Rev., 121, 3040-3061

Tiedtke M, Klinker E, Kvamsto N-G, Morcrette J-J, Rizzi and Vesperini (1993) Cloud and Radiation Modelling at ECMWF. IAMAP International Workshop on Cloud-Radiation Interactions. NOAA, Science Center, Camp springs, MD, 18-20 October 1993.